ACADEMIC PRESS

Available online at www.sciencedirect.com

SCIENCE DIRECT®

Journal of Magnetic Resonance 164 (2003) 54–59

JMR Journal of Magnetic Resonance

www.elsevier.com/locate/jmr

An improved external loop resonator for in vivo L-band EPR spectroscopy

Ildar Salikhov,[a,1] Hiroshi Hirata,[b] Tadeusz Walczak,[a] and Harold M. Swartz[a,*]

[a] *EPR Center for the Study of Viable Systems, Department of Diagnostic Radiology, Dartmouth Medical School, Hanover, NH 03755, USA*
[b] *Department of Electrical Engineering, Yamagata University, Yonezawa, Yamagata 992-8510, Japan*

Received 21 January 2003; revised 7 May 2003

Abstract

An improved external loop resonator (ELR) used for L-band electron paramagnetic resonance (EPR) spectroscopy is reported. This improvement is achieved by shortening the parallel coaxial line. The resonant structure is formed by two single turn coils (10 mm in diameter) that are connected to a parallel coaxial line. A resonance frequency of 1197 MHz and a quality factor of 466 were obtained in the absence of biological tissue and ~1130 MHz and ~50 with a living animal, respectively. The sensitivity of the new ELR was compared to the previously developed ELR using three types of EPR samples: (1) paramagnetic material with no biological tissue, (2) paramagnetic material in a leg and in the peritoneal cavity of a dead rat, and (3) paramagnetic material in the back of an anesthetized rat. The sensitivity was 1.2–1.6 times greater in the rat and 4.2 times without tissue.

Keywords: Surface coil; Signal-to-noise ratio; Resonance frequency; Biological tissue; Continuous-wave EPR spectroscopy

1. Introduction

The sensitivity of an electron paramagnetic resonance (EPR) spectrometer is one of the most important aspects for productive biomedical EPR studies. The microwave resonator is a key element for achieving high sensitivity with EPR in living subjects. Surface-coil-type resonators have been especially productive, facilitating localized measurements without acute invasion. We especially have used external loop resonators (ELR) to measure oxygen-sensitive paramagnetic samples such as microcrystals of lithium phthalocyanine (LiPc) implanted at the site of interest [1–16]. This can provide very useful information on oxygen-dependent physiological and pathological processes [17–19].

The previously developed ELR [9] had a resonance frequency of ~1200 MHz. It consisted of a single-turn external coil, 10 mm in diameter, connected to an approximately half-wavelength (84 mm) parallel transmission line connected to the gap of a coupled two-loop-one-gap resonator with 10 mm diameter loops. One of these loops was inductively coupled to a 50-Ω line by a coupling loop of the same diameter, connected to the line by a twisted pair cable. To further improve the sensitivity of the ELR, we tested a resonator of similar design with the same diameter external loop, but with a decreased length of the parallel line and with a single turn loop instead of a loop-gap resonator. This paper reports a design of the modified ELR, the calculation of the resonance frequency, the comparison of the sensitivity of the previously developed and modified ELRs, and a discussion of results.

2. Method

2.1. Construction and characterization of resonator

Fig. 1 is a schematic diagram of the newly developed ELR. It consists of a segment of a 29-mm long transmission line, formed by two parallel 50-Ω coaxial lines and two 10 mm diameter single-turn coils made from 0.8 mm silver plated wire and connected by ~4 mm and

* Corresponding author. Fax: 1-603-650-1717.
E-mail address: harold.swartz@dartmouth.edu (H.M. Swartz).
[1] Also corresponding author.

1090-7807/$ - see front matter © 2003 Elsevier Science (USA). All rights reserved.
doi:10.1016/S1090-7807(03)00175-7

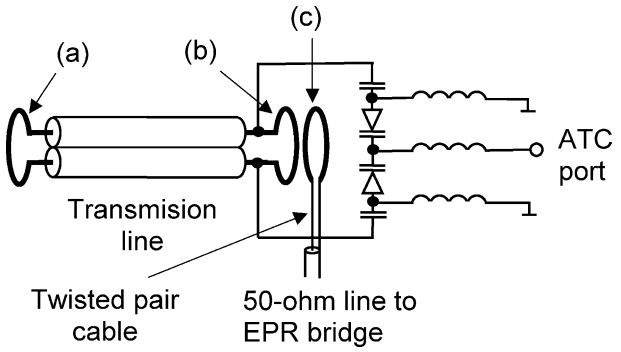

Fig. 1. Schematic diagram of the newly developed external loop resonator (ELR). The parallel coaxial line is formed with 50-Ω commercially available semi-ridged coaxial lines. The outer diameter of the coaxial line was 6.2 mm. The diameter of the external and internal coils was 10 mm, both loops had ~3 mm gap and the thickness of the wire was 0.8 mm. The length of the wires connecting the external and internal loops to the parallel line was ~4 and ~6 mm, respectively. The length of the parallel line was 29 mm. The length of the twisted pair cable was adjusted to reduce shifts in the resonance frequency due to changes of the coupling [20].

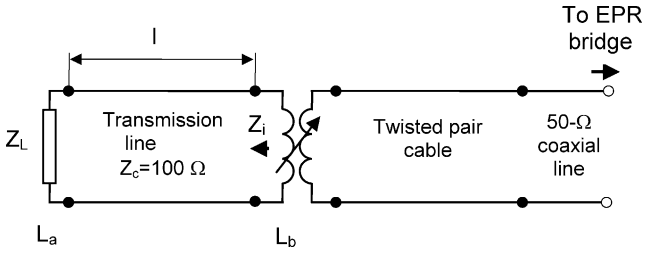

Fig. 2. Equivalent circuit of the main resonant circuit in the newly developed ELR. The impedances of the external loop Z_L and the internal loop are connected to the parallel transmission line (the characteristic impedance was 100 Ω).

~6 mm long wires to both ends of the line. Both coils had a ~3 mm gap. One single-turn coil called the external loop ('a' in Fig. 1) is used to deliver the RF magnetic field to the sample, and the other coil called the internal loop ('b' in Fig. 1) is inductively coupled with a coupling loop ('c' in Fig. 1) to transmit the microwave power from the bridge to the resonator. The impedance matching between the resonator and the 50-Ω coaxial line is adjusted by changing the distance between coils (b) and (c) as in a standard inductive coupling. The coupling coil (c) is connected to the coaxial line by a twisted pair cable, and the length of this twisted pair cable is adjusted to reduce the shift in the resonance frequency [20]. Varactors connected to the parallel line through capacitors are used for automatic tuning control (ATC) and choke coils are used for decoupling the voltage-control circuits of the varactors. A gold-plated brass shielding case isolates the coupling and tuning circuits of the resonator from magnetic field modulation.

The resonance frequencies and quality factors of the critically coupled ELRs were measured with a network analyzer (Hewlett Packard, Palo Alto, CA, 8753A). Measurements were done in parallel with recording of EPR spectra keeping the same distance between the loop and tissue.

2.2. Resonance frequency estimation

Designing resonators is facilitated by having knowledge of the resonance frequency. Fig. 2 shows an equivalent electrical circuit for the new ELR, and this allowed us to calculate the resonance frequency. The imaginary part of the input impedance Z_i of the parallel line connected to the external loop with inductance L_a depends on the inductance of the coil and the length of the line. When the input impedance is capacitive, it can be a part of the resonant circuit by connecting an inductive element—internal loop with inductance L_b to parallel line. The resonance condition of this system is given by

$$\mathrm{Im}[Z_i] + \omega L_b = 0, \tag{1}$$

The input impedance Z_i is calculated by

$$Z_i = Z_c \frac{Z_L + jZ_c \tan \beta l}{Z_c + jZ_L \tan \beta l}, \tag{2}$$

where Z_c is the characteristic impedance of the parallel line (100 Ω), ω is the angular frequency, $Z_L = j\omega L_a$ is the impedance of the load of the line (the impedance of the external loop), l is the length of the line, $\beta = 2\pi/\lambda$ is the phase constant of the line (λ is the wavelength in the line, $\beta = 36.4$ rad/m at 1.2 GHz), and j is the imaginary number unit. While the external loop has radiation, ohmic, and dielectric losses in biological tissues, those losses can be ignored when estimating the resonance frequency. Attenuation of the parallel transmission line also was neglected. These factors for energy dissipation are, however, important in estimating the quality factor and the efficiency for generating the RF magnetic field.

To determine the frequency satisfying the resonance condition given in Eq. (1), we used the Newton method in numerical computations. While the coupling loop affects the resonance frequency of the resonator, we neglected the influence of the mutual coupling between two coils since this influence was relatively small (in the range of few MHz). If a more precise estimate of the resonance frequency were necessary, the neglected factors would need to be considered. Since external/internal coil is not a complete circle and the coil has connecting wires with additional inductance, we estimated inductance of such a coil with connecting wires as inductance of complete circle coil with length of circumference equal to length of wire of loop with diameter d and with gap g plus lengths l_w of two connecting wires. The diameter D and the inductance of such a coil made from wire with diameter a is given by $(\pi d - g + 2l_w)/\pi$ and

$0.5D\mu_0\mu[\ln(8D/a) - 2]$, respectively, where μ_0 and μ are the absolute permeability and relative permeability of media, respectively.

2.3. Comparison of sensitivities

Sensitivities of the ELRs were compared with our L-band spectrometer, using the same paramagnetic samples and the same settings of the EPR spectrometer. There was no saturation of the EPR signal in all measurements. The RF power applied to the resonator, the scan width, the amplitude of magnetic field modulation, and the time constant of a lock-in amplifier were 20 mW, 1.5–3.0 mT (scan width was same for each pair of spectra obtained from same sample with old and new resonators), 0.04 mT and 30 ms, respectively. The root-mean-square (RMS) value of the noise amplitude was measured with a computer program incorporated into the main control program of the EPR spectrometer. All EPR spectra were recorded with an ATC system that adjusted the resonance frequency of a resonator to the frequency of the microwave oscillator.

To compare sensitivities of the resonators we used three types of samples: (1) a small amount of 1,1-diphenyl-2-picrylhydrazyl (DPPH) powder in a plastic holder, (2) a point sample of DPPH in tissues with three different levels of loss: (2a) the leg of a dead male Sprague–Dawley rat weighting ~250 g, (2b) a cylindrically cut piece of bovine skeletal muscle (50 mm in diameter and 40 mm in length) in a plastic holder, (2c) the peritoneal cavity of the dead rat with DPPH injected in the center of the abdomen, and (3) a char in the middle of the surface of the back of an a live ~250 g male Sprague–Dawley rat anesthetized with 1.25% isoflurane. The measurements without tissue gives the sensitivity of the ERL without the significant electromagnetic loss that can occur with biological tissue. EPR measurements of an extracted tooth are close to this model. The second and third models are more typical for most biomedical applications, testing the sensitivity of the ELR with lossy biological tissues. The measurements with the third model includes both perturbations due to the motions of an animal and eddy current losses in biological tissue; this is a reasonable experimental model for biomedical applications. The resonator was positioned so that the EPR sample was located on the axis of the external loop for all of the EPR measurements.

To compare the sensitivities of the resonators, it was necessary to control the position of the surface loop with respect to the position of the EPR signal source and also to the tissue when switching between resonators. The comparisons of the sensitivities without tissue and with bovine skeletal muscle were carried out with a low-loss plastic holder for the paramagnetic materials. The holder provided a precise positioning of the DPPH in the center of the loop and a constant distance of 0.5 mm between the loop and the sample. In the absence of biological tissue, the holder with DPPH was secured to the loop. For the measurements of bovine skeletal muscle, the DPPH was positioned on the surface of the tissue, concentrically with the axis of the surface loop and the cylindrical holder of tissue. For the measurements in rats, similar amounts of DPPH were injected at a depth of 2–3 mm for the leg and 3–5 mm for the peritoneal cavity.

The effect of the motions of an animal in both resonators was compared by recording EPR spectra from a small piece of char that was glued to the surface of the back of a living rat, over the region of the moving lungs. Experiments were done with an ATC in which the resonance frequency of the resonator was locked by varactors to the frequency of the oscillator of the bridge; consequently the frequency of the oscillator was not affected by the motion of the animal and therefore there was no change in the resonance position of the EPR line, which could have resulted in a distorted lineshape of the narrow line. On the other hand, a high modulation level can shift the base line due to microphonics; the amplitude of this shift depends on the occurrence of mismatching of the resonator due to motion of the animal. Such mismatches can cause spikes in both the baseline and EPR signal. Those spikes would be additional to spikes in the EPR line caused by changes of the amplitude of the EPR line amplitude due to changes in the distance between the loop and the paramagnetic sample. Since using a broader EPR line makes it feasible to use a higher amplitude of modulation, we used a char with a linewidth 0.5 mT instead of DPPH to test the impact of animal motion on EPR spectra, employing experimental conditions that were especially sensitive to the motions of an animal. Therefore the applied RF power and modulation amplitude were increased to 80 mW and 0.2 mT, respectively. The scan width and the time constant of the lock-in amplifier were 4.0 mT and 30 ms, respectively.

3. Results and discussion

3.1. Resonance frequencies and quality factors

The resonance frequency of a critically coupled resonator without varactors was 1274 MHz. Addition of a tuning circuit with varactors decreased the resonance frequency to 1197 MHz. When the external loop was adjacent to the peritoneal cavity of the rat, the resonance frequency was decreased to 1130 MHz.

Fig. 3 shows the results of the numerical computations for the resonance frequency as a function of the length of the parallel transmission line and diameter of the external loop (7, 10, and 15 mm) for the loop with a 10-mm internal diameter loop. When the length of the

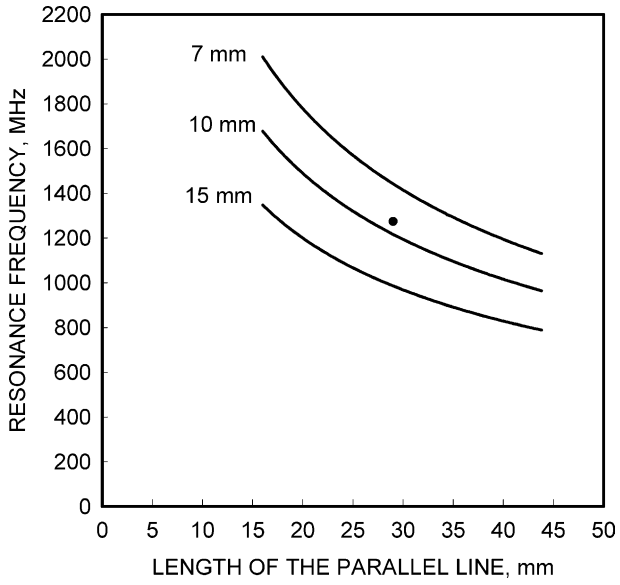

Fig. 3. Calculated resonance frequency of new ELR as a function of the length of the parallel line and the diameter of the external loop, with an internal loop of 10 mm in diameter (solid lines). The numerical calculations were carried out with the Newton method to find the resonance condition given in Eq. (1). The closed circle shows the measured resonance frequency of a prototype ELR with a 29-mm long line: 1262 MHz in the absence of tuning capacitors and tissue.

transmission line was 29 mm and the estimated inductance of the 10 mm in diameter loop with 3 mm gap and with 4 and 6 mm long connecting wires is 20.0 and 23.1 nH, respectively, the calculated resonance frequency of the prototype ELR was 1216 MHz, which is close to the experimentally obtained resonance frequency of 1274 MHz for the case of no varactors and biological tissue. This indicates the validity of the equivalent circuit in Fig. 2 and the formulas used to estimate the resonance frequency.

In the models with biological tissue, the quality factors of the new ELR were in the range 50–60 (see Table 1). The resultant quality factors are less than a half of those of the previously developed ELRs quality factors.

3.2. Amplitudes of EPR signals and noise

The experimental data on amplitudes of EPR spectra indicate that the new resonator provides up to a 4.2-fold improvement of sensitivity in the absence of tissue adjacent to the external loop, as shown in Fig. 4. This is a remarkable improvement for the signal-to-noise ratio with significant impact on EPR instrumentation. However, the improvement in sensitivity is smaller when there are tissues adjacent to the loop of the resonator.

When the paramagnetic material was in the leg or in peritoneal cavity of the rat the lineshapes of the first derivative EPR absorption curves were asymmetric, due to phase shift in the conducting media. The phase shift for the spectra from the material in the peritoneal cavity was larger than that for bovine skeletal muscle, due to the deeper location of the paramagnetic material.

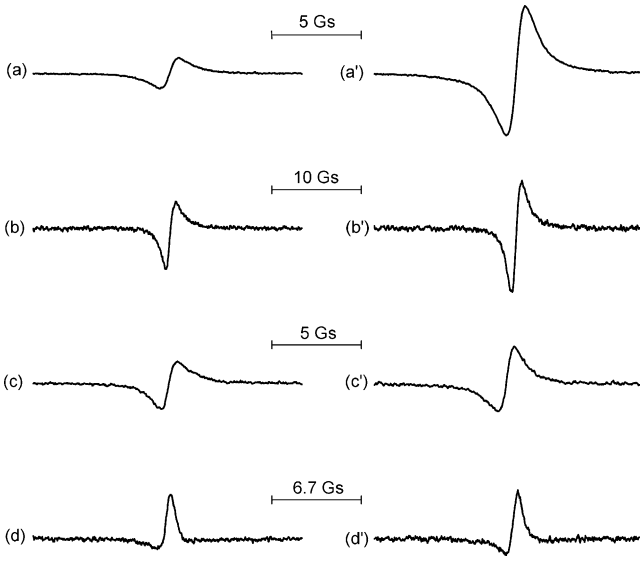

Fig. 4. EPR spectra of 1,1-diphenyl-2-picrylhydrazyl (DPPH) measured with the new and conventional ELRs in air and in tissues. Spectra (a) and (a′) were measured with a point sample of DPPH in plastic holder without biological tissue. Spectra (c) and (c′) also were measured with the DPPH in same plastic holder, which was placed on a cylindrically cut piece of bovine skeletal muscle (50 mm in diameter and 40 mm in length). A point sample of DPPH was implanted in a leg, (b) and (b′), and the peritoneal cavity of a dead male Sprague–Dawley rat weighting 240 g, (d) and (d′). The spectra on the left were obtained with the conventional ELR, and those on the right were made with the new ELR. Each pair of spectra was measured at the same settings of the EPR spectrometer: the scan width was 1.5–3.0 mT, the field modulation was 0.04 mT, the scan time was 10 s, the time constant was 30 ms, and the applied RF power was 20 mW.

Table 1
Quality factors and the ratios of peak-to-peak amplitudes of EPR signals of 1,1-diphenyl-2-picrylhydrazyl (DPPH) obtained with the new and conventional external loop resonators with and without biological tissues

Tissue adjacent to loop of resonator	Quality factor of the resonator		Ratio of EPR signal amplitudes with new and conventional resonators
	New	Conventional	
No tissue	466	500	4.2
Rat–leg	60	162	1.6
Isolated bovine muscle	62	157	1.4
Rat–peritoneal cavity	49	95	1.2

While bovine skeletal muscle is also a conductive medium, there was no significant phase shift in the spectrum, because the paramagnetic material was on the surface of the tissue. The amplitude of the noise for each pair of measurements with the two resonators was the same, within 15% of RMS noise amplitude.

Table 1 summarizes the quality (Q) factors and the ratios of the EPR signal amplitudes in four models with the new and conventional ELR. The higher amplitude of the EPR signal of the new resonator at the same level of applied RF power suggests that the new resonator has a better efficiency for generating the RF magnetic field [21]. In addition, the experimental data of Fig. 4 and Table 1 suggest that a higher amplitude of the signal has been achieved with a similar (no tissue) or even lower (with tissue adjacent to loop) Q-factor of the new resonator. Since the amplitude of the signal is proportional to the product ηQ (see e.g., [22]), where η is the filling factor of the resonator, the experimental data suggest that the filling factor for the new resonator is higher, compared to the previous resonator. Indeed, since the external loops of both resonators had the same diameter, the shorter parallel transmission line and simple 1-turn internal loop of the new resonator should store relatively less of the total energy of the resonator than the longer parallel transmission line and the internal 2-loop-one-gap coupling structure of the old resonator. Therefore, the external loop of the new resonator should have a relatively larger part of the total energy stored in resonator. Also, the losses apparently were smaller in the shorter parallel line. The higher energy in the loop of with the same diameter results in a higher H_1 in sample. That should result both in better efficiency and a better filling factor in the new resonator. The improvement of signal intensity is greatest in the case of no tissue. However, if there is material with a high dielectric constant such as tissues adjacent to the loop, the increased efficiency increases the dissipation of the energy due to radiation of the electromagnetic energy to free space [16] and losses in tissue. Therefore the quality factor of the new resonator is smaller and the increase of the sensitivity due to the higher filling factor is partially offset by this drop of the quality factor (see b, b′, c, c′, d, and d′ on Fig. 4). Using such a resonator in biological samples that are less lossy, such as teeth for dosimetry [23], could result in a larger increase in sensitivity.

Since the newly developed resonator with lossy tissue provides slightly better EPR signal amplitude at lower Q-factor, the resonator has the additional potential for improvement of sensitivity of EPR spectrometer as the broader bandwidth of the new resonator decreases the conversion of the phase noise of the microwave oscillator (better than −120 dBc/Hz @ 100 kHz in our case) in the EPR spectrometer into amplitude noise. That should result in a better signal-to-noise ratio at a high level of RF power, where the phase noise of the oscillator usually makes the main contribution to total noise. In our experiments RF power level was not high enough to see a difference in noise level with new and old resonators.

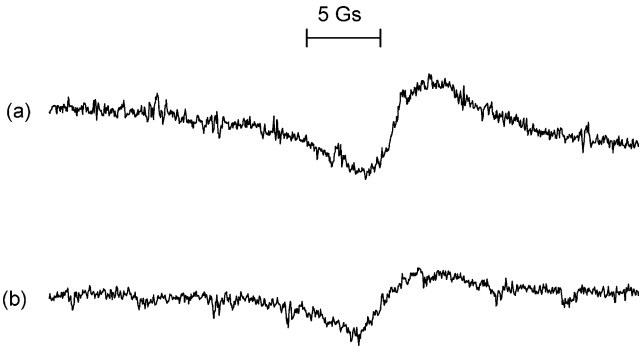

Fig. 5. EPR spectra of a char on the surface of the back of a live male 250 g Sprague–Dawley rat anesthetized with 1.25% isoflurane and measured with the newly developed ELR (a), and with the conventional ELR (b). For both measurements, the parameters in the EPR spectrometer were the same: the applied RF power was 80 mW, the amplitude of field modulation was 0.2 mT, the scan width was 4.0 mT, and the time constant of the lock-in amplifier was 30 ms.

Even in the situation with the presence of tissues and hence higher losses, the improvement of sensitivity of 20–60% could be very useful, especially because some biomedical measurements need to be carried out in a short time due to physiological changes that occur fairly rapidly.

EPR spectra measured from a char in an anesthetized rat showed similar amplitudes of spikes due to the motions of an animal (Fig. 5). That indicates the ATC system is still able to compensate for shifts in the resonance frequency due to the motions of an animal, while the new ELR is more sensitive to the perturbation. Since suppression of spikes due to motion depends on both the resonator and the characteristics of the ATC system, the issue of the robustness for the motions of an animal requires further considerations.

4. Conclusions

The sensitivity of a newly developed ELR was compared with that of the previously developed ELR, and an improvement up to 4.2 times of the sensitivity has been achieved. A comparison of the sensitivities of the resonators in biological samples (isolated bovine muscle, rat's peritoneal cavity and leg) with significant electromagnetic losses showed a smaller but still significant improvement of the signal-to-noise ratio, of 1.2–1.6 times. These results indicate that a decrease of the length of the parallel line of these resonators increases the magnetic energy stored in the external loop and improves sensitivity.

Acknowledgments

The authors are grateful to Dr. H. Hou and Dr. P. Hein for their help in the animal experiments. This work was supported by NIH Grant P41EB002032 (to H.M.S.) and a Grant (12750377) from the Japan Society for the Promotion of Science and Technology (to H.H.).

References

[1] J.J.H. Ackerman, T.H. Grove, G.G. Wong, D.G. Gadian, G.K. Radda, Mapping of metabolites in whole animals by ^{31}P NMR using surface coils, Nature 283 (1980) 167–170.
[2] O.C. Morse, J.R. Singer, Blood velocity measurements in intact subjects, Science 170 (1970) 440–441.
[3] M. Garwood, T. Schleich, G.B. Mattson, Spatial localization of tissue metabolites by phosphorus-31 NMR rotation-frame zeugmatography, J. Magn. Reson. 60 (1984) 268–279.
[4] H. Nishikawa, H. Fujii, L.J. Berliner, Helices and surface coils for low-field in vivo ESR and EPR imaging applications, J. Magn. Reson. 62 (1985) 79–86.
[5] C. Kroll, W. Herrmann, R. Stober, H.H. Borchert, K. Mader, Influence of drug treatment on the microacidity in rat and human skin: an in vitro electron spin resonance imaging study, Pharmaceut. Res. 18 (2001) 525–530.
[6] J. Fuchs, N. Groth, T. Herrling, G. Zimmer, Electron paramagnetic resonance studies on nitroxide radical 2,2,5,5-tetramethyl-4-piperidin-1-oxyl (TEMPO) redox reactions in human skin, Free Radical Biol. Med. 22 (1997) 967–976.
[7] G. He, A. Samouilov, P. Kuppusamy, J.L. Zweier, In vivo EPR imaging of the distribution and metabolism of nitroxide radicals in human skin, J. Magn. Reson. 148 (2001) 155–164.
[8] S. Petryakov, M. Chzhan, A. Samouilov, G. He, P. Kuppusamy, J.L. Zweier, A bridged loop-gap S-band surface resonator for topical EPR spectroscopy, J. Magn. Reson. 151 (2001) 124–128.
[9] H.M. Swartz, F. Goda, T. Walczak, K.J. Liu, U.S. patent 5,494,030, 1996.
[10] P. Turek, J.-J. Andre, A. Giraudeau, J. Simon, Preparation and study of a lithium phthalocyanine radical: optical and magnetic properties, Chem. Phys. Lett. 134 (1987) 471–476.
[11] K.J. Liu, P. Gast, M. Moussavi, S.W. Norby, N. Vahidi, T. Walczak, M. Wu, H.M. Swartz, Lithium phthalocyanine: a prove for electron paramagnetic resonance oximetry in viable biological systems, Proc. Natl. Acad. Sci. USA 90 (1993) 5438–5442.
[12] G. Ilangovan, J.L. Zweier, P. Kuppusamy, Electrochemical preparation and EPR studies of lithium phthalocyanine: evaluation of the nucleation and growth mechanism and evidence for potential-dependent phase formation, J. Phys. Chem. B 104 (2000) 4047–4059.
[13] G. Ilangovan, J.L. Zweier, P. Kuppusamy, Electrochemical preparation and EPR studies of lithium phthalocyanine. Part 2: particle-size-dependent line broadening by molecular oxygen and its implications as an oximetry probe, J. Phys. Chem. B 104 (2000) 9404–9410.
[14] G. Ilangovan, H.Q. Li, J.L. Zweier, P. Kuppusamy, Electrochemical preparation and EPR studies of lithium phthalocyanine. 3: measurements of oxygen concentration in tissues and biochemical reactions, J. Phys. Chem. B 105 (2001) 5323–5330.
[15] H. Hirata, T. Walczak, H.M. Swartz, Electronically tunable surface-coil-type resonator for L-band EPR spectroscopy, J. Magn. Reson. 142 (2000) 159–167.
[16] H. Hirata, T. Walczak, H.M. Swartz, Characteristics of an electronically tunable surface-coil-type resonator for L-band electron paramagnetic resonance spectroscopy, Rev. Sci. Instrum. 72 (2001) 2839–2941.
[17] P.E. James, O.Y. Grinberg, F. Goda, T. Panz, J.A. O'Hara, H.M. Swartz, Gloxy: an oxygen-sensitive coal for accurate measurement of low oxygen tensions in biological system, Magn. Reson. Med. 38 (1998) 48–58.
[18] J. He, N. Beghein, R.B. Clarkson, H.M. Swartz, B. Gallez, Microencapsulation of carbon particles used as oxygen sensors in EPR oximetry to stabilize their responsiveness to oxygen in vitro and in vivo, Phys. Med. Biol. 46 (2001) 3323–3329.
[19] O.Y. Grinberg, A.I. Smirnov, H.M. Swartz, High spatial resolution multi-site EPR oximetry, J. Magn. Reson. 152 (2001) 247–258.
[20] H. Hirata, T. Walczak, H.M. Swartz, An improved inductive coupler for suppressing a shift in the resonance frequency of electron paramagnetic resonance resonators, Rev. Sci. Instrum. 68 (1997) 3187–3191.
[21] J.S. Hyde, W. Froncisz, T. Oles, Multipurpose loop-gap resonator, J. Magn. Reson. 82 (1989) 223–230.
[22] G.A. Rinard, R.W. Quine, J.R. Harbridge, R. Song, G.R. Eaton, S.S. Eaton, Frequency dependence of EPR signal-to-noise, J. Magn. Reson. 140 (1999) 218–227.
[23] M. Miyake, K.J. Liu, T. Walczak, H.M. Swartz, In vivo EPR dosimetry of accidental exposures to radiation: experimental results indicating the feasibility of practical use in human subjects, Appl. Radiat. Isot. 52 (2000) 1031–1038.